Polymer 51 (2010) 4843–4849

Contents lists available at ScienceDirect

Polymer

journal homepage: www.elsevier.com/locate/polymer

The preparation of high performance silk fiber/fibroin composite

Qingqing Yuan, Jinrong Yao, Xin Chen, Lei Huang, Zhengzhong Shao*

The Key Laboratory of Molecular Engineering of Polymers of MOE, Department of Macromolecular Science, Laboratory of Advanced Materials, Fudan University, Shanghai, 200433, PR China

ARTICLE INFO

Article history:
Received 21 April 2010
Received in revised form
17 August 2010
Accepted 19 August 2010
Available online 24 August 2010

Keywords:
Animal silk
Surface modification
Compatibility

ABSTRACT

An all-silk composite, in which uniaxially-aligned and continuous-typed *Bombyx mori* silk fibers were embedded in a matrix of silk protein (fibroin), was successfully prepared via a solution casting process. The structure, morphology, mechanical and thermal properties of such silk fiber/fibroin composites were investigated with X-ray diffraction, scanning electron microscopy, tensile and compression tests, dynamic mechanical analysis and thermogravimetric analysis. The results demonstrated that the interface adhesion between silk fiber and the fibroin matrix was enhanced by controlling the fiber dissolution through 6 mol L^{-1} LiBr aqueous solution. Compare to those of the pure fibroin counterparts, the overall mechanical properties as well as the thermal stability of such silk fiber/fibroin composites were significantly improved. For example, the composite with 25 wt% fibers showed a breaking stress of 151 MPa and a breaking elongation of 27.1% in the direction parallel to the fiber array, and a compression modulus of 1.1 GPa in the perpendicular direction. The pure fibroin matrix (film), on the other hand, typically had a breaking stress of 60 MPa, a breaking elongation of 2.1% and a compression modulus of 0.5 GPa, respectively. This work suggests that such a controllable technique may help in the preparation of animal silk based materials with promising properties for various applications.

1. Introduction

In the past decades, growing emphasis on environmental concerns and exhausting depletion of petroleum sources have triggered the exploration of natural fibers as a "green" alternative for synthetic polymer fibers in composites. Because of their advantages such as low cost, low density, renewability, biodegradability and acceptable specific strength etc., a bulk of natural fibers have been utilized for structural/semi-structural materials in various fields including aerospace, automotive, building, furniture, packaging and sports articles. However, most of them are originated from lignocellulosic fibers [1–3].

Bombyx mori silkworm silk, a representative animal fiber of luster and fineness, has been used in the textile industry for centuries. It structurally consists of a fibrous core protein named fibroin, and a family of glue-like proteins named sericin that surround the fibroin threads to cement them together. The high crystallinity of β-sheets (ca. 50%) as well as the well orientation of these nanocrystallites in the core filament [4] gives silkworm silk the remarkable mechanical properties, especially strength (0.4 GPa) and extensibility (20%) [5,6]. In addition, the homogeneous physicochemical properties of silkworm silk as a continuous fiber allow for the fabrication facilities via filament winding and pultrusion processes. Recently, silkworm silk has received great interest as a filling material in composites. For example, chopped silk and commercial silk fabric have been used to reinforce biodegradable or synthetic polymers such as poly(butylene succinate) [7,8], poly(ε-caprolactone) [9], poly(lactic acid) [10], or even polychloroprene rubber [11]. However, chopped silk loses the mechanical merits as a continuous fiber, and commercial silk fabric suffers from the wetting problem of twisted fibroin threads in the matrix, both of which may result in the uncompetitive mechanical performance of the reported silk composites.

It is well known that the adhesion between components (e.g. the fiber phase and the matrix phase) is crucial for the mechanical performance of a composite. On one hand, Jin et al. [8] modified silk fabric with carbon nanotubes to improve its compatibility with poly[(butylene succinate)-co-(butylene adipate)], and obtained a composite with fairly increased mechanical properties. On the other hand, Li et al. [12] directly composed silk fabric with regenerated silk fibroin (RSF); however, the overall mechanical properties of the composite were still unsatisfactory. This was likely caused by the immiscibility between the different fine structures of silk fibroin, i.e., the well-ordered β-sheet in silk fiber [13] and either the amorphous state [14] or the randomly-aligned β-sheet [15] in

* Corresponding author. Tel.: +86 21 65642866; fax: +86 21 65640293.
E-mail address: zzshao@fudan.edu.cn (Z. Shao).

0032-3861/$ – see front matter © 2010 Elsevier Ltd. All rights reserved.
doi:10.1016/j.polymer.2010.08.042

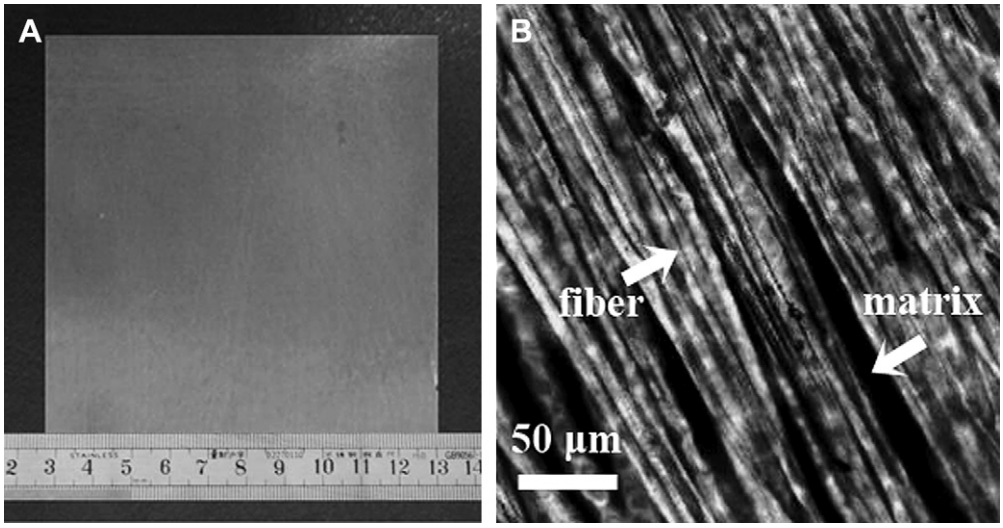

Fig. 1. Photograph (A) and POM image (B) of Composite-5.

RSF matrix. Furthermore, due to the highly-repeating GAGAGS (G = glycine, A = alanine and S = serine) motifs and the highly-ordered structure, silk fiber presents a water-resistant feature [16] that indicates its inadequate wettability with RSF solution. Since partial fiber dissolution (either by solvent or by thermal melting) seems a straightforward approach to prepare fiber composites with good interface adhesion [3,17–20], a moderate concentration of LiBr aqueous solution (i.e. 6 mol L^{-1}) was applied on silk fiber to improve its adhesion with RSF matrix in this work. Therefore, a robust and tough all-silk composite was successfully produced by embedding the LiBr-pretreated silk fibers in alignment to the high concentration of RSF aqueous solution and through an eco-friendly solution casting process.

2. Experimental section

2.1. Preparation of silk fiber/fibroin composites

B. mori cocoon silk was degummed in 0.5 wt% $NaHCO_3$ aqueous solution to remove sericin [14]. The degummed silk fibers were then dissolved in 9.5 mol L^{-1} LiBr aqueous solution. After being filtered, the fibroin solution was dialyzed against deionized water for three days at room temperature with a 12–14 kDa cutoff semi-permeable membrane to remove the salt. The dialyzed solution was centrifuged and the supernatant was concentrated to 15 wt% solution according to the established procedures [21]. The 15 wt% fibroin solution was stored at 4 °C and further used for the regenerated silk fibroin (RSF) matrix.

The preparation method of silk fiber/fibroin composites was the subject of our Chinese patent application [22] and the typical process was as below: A uniform layer of silk fibers was achieved by reeling fibroin threads from *B. mori* cocoons directly onto a cylindrical spool by a homemade reeling machine. With both ends fixed, the uniaxially-aligned fibers were degummed in 0.5 wt% $NaHCO_3$ aqueous solution to remove sericin. Then various amounts of the degummed fibers were treated by 6 mol L^{-1} LiBr aqueous solution for 10 min, rinsed repeatedly with deionized water, and finally impregnated in 15 wt% RSF solution at 4 °C prior to completely cast at room temperature and 50 ± 5% RH. The air-cast composite films were vacuumed under room temperature and kept in a desiccator before the measurements. Such silk fiber/fibroin composites were briefly marked Composite-X, and X was the mass percentage of silk fibers in the composites.

2.2. Structure and morphology characterizations

The polarized optical microscopy (POM) image of Composite-5 was taken by Olympus BX51 research microscope.

The scanning electron microscope (SEM) images of the longitudinal and transverse fracture sections of gold sputtered Composite-20 were observed using Tescan 5136 MM scanning electron microscope at an accelerating voltage of 20 kV.

X-ray diffraction patterns were recorded on PANalytical X'Pert PRO diffractometer at 40 kV and 40 mA with Cu K_α radiation.

2.3. Mechanical property measurements

Tensile and compression tests were both carried out on Instron 5565 universal test machine at room temperature and 50 ± 5% RH. In the tensile test, the specimen dimensions were 100 mm × 5 mm × (0.2 ± 0.05) mm, the gauge length was 20 mm, and the tensile rates in the directions parallel and perpendicular to the fiber array were 2 and 0.2 mm min^{-1}, respectively. In the compression test, a pile of composite films (10 mm × 10 mm × 0.2 mm) were applied as the specimen with a compression height of ca. 2 mm and a crosshead rate of 0.2 mm min^{-1}. The results obtained from the tensile and compression tests were averaged by 10 and 5 measurements, respectively.

2.4. Dynamic mechanical analysis (DMA)

The dynamic mechanical tests of Composite-20 and pure RSF matrix were performed on Netzsch 242 dynamic mechanical analyzer after preheating at 130 °C for 15 min to remove moisture. The dynamic mechanical test of degummed silk fiber was performed on Rheometric Scientific DMTA IV with a more sensitive load sensor. All the tests were carried out with 1 Hz of frequency, 0.5% of strain and 3 °C min^{-1} of heating rate [23].

2.5. Thermogravimetric analysis (TGA)

The thermal stability of composites with different fiber content as well as pure RSF matrix and degummed silk fiber was examined up to 700 °C through Perkin Elmer Pyris-1 thermogravimetric analyzer at a heating rate of 10 °C min^{-1}. A purging nitrogen gas stream of 40 mL min^{-1} was used.

Table 1
Comparison of the overall mechanical properties of silk fiber/fibroin composites with RSF matrix.

	Tensile[a]				Compression[b]
	Breaking stress (MPa)	Breaking elongation (%)	Tensile modulus (GPa)	Breaking energy[c] (kJ kg^{-1})	Compression modulus (GPa)
RSF matrix	60 ± 8	2.1 ± 0.2	3.7 ± 0.4	0.5 ± 0.1	0.5 ± 0.1
Composite-10	83 ± 7	11.2 ± 1.3	3.1 ± 0.2	5.5 ± 1.0	0.7 ± 0.1
Composite-20	142 ± 7	23.5 ± 1.7	3.0 ± 0.2	18.6 ± 1.8	1.0 ± 0.1
Composite-25	151 ± 5	27.1 ± 1.4	2.8 ± 0.1	23.2 ± 1.9	1.1 ± 0.1

[a] Tensile test was performed in the direction parallel to the fiber array.
[b] Compression test was performed in the direction perpendicular to the fiber array.
[c] Breaking energy was calculated by the area under the tensile stress–strain curve, with the density of silk fibroin employed as 1.3 g cm^{-3} [26].

3. Results

3.1. Mechanical properties

Animal silk (from either silkworm or spider), is a one-dimensional material with excellent mechanical properties, but has few applications for three-dimensional materials except for the woven textile. The current silk protein materials such as RSF film were commonly produced from the regenerated silk protein solution at expense of the fiber merits (e.g. remarkable tensile properties) [24,25]. Therefore, enhancing the brittle RSF matrix with silk fiber can lead to a high performance all-silk composite with desired good compatibility.

As shown in Fig. 1A, the silk fiber/fibroin composite film had a homogeneous composition, with a size of 100 mm × 100 mm and a thickness of 0.1–0.5 mm depending on the fiber quantity. The POM image of Composite-5 (Fig. 1B) revealed that the uniform alignment of silk fibers was well preserved in RSF matrix, even after a series of sericin degumming, LiBr pretreatment, matrix embedment and solution casting.

Table 1 showed that the produced silk fiber/fibroin composites possessed well combination on mechanical characteristics. For the tensile test in the direction parallel to the fiber array, the average breaking stress and breaking elongation of Composite-10 were 83 MPa and 11.2%, respectively, and even approached 151 MPa and 27.1% for Composite-25, which were much better than those of pure RSF matrix (60 MPa and 2.1%). Especially, the breaking energy was greatly enhanced with the increase of fiber content, e.g. 23.2 kJ kg^{-1} for Composite-25 vs. 0.5 kJ kg^{-1} for the matrix. It indicated that the brittle RSF matrix was toughened by silk fiber in the parallel direction. But interestingly, the tensile modulus of the composites was slightly decreased (e.g. 2.8 GPa for Composite-25 vs. 3.7 GPa for the matrix), which was likely caused by the reduction of fibroin density at the fiber/matrix interface. Besides, the compression test revealed that the brittle RSF matrix was also reinforced in the perpendicular direction as the compression modulus of Composite-25 was twice as strong as that of pure RSF matrix, i.e. 1.1 GPa vs. 0.5 GPa. Therefore, it was concluded that the overall mechanical properties of RSF matrix were gradually enhanced with the incorporation of the LiBr-pretreated silk fibers up to 25 wt%.

3.2. XRD results

In Fig. 2, pure RSF matrix displayed only a broad and weak scattering peak centered at around 20°, indicating a predominantly amorphous conformation. Silk fiber displayed a representative main diffraction peak at 20.6° as well as a small peak at about 9.4°, both of which were attributed to the high crystallinity of anti-parallel β-sheet conformation [27]. The two β-sheet diffraction peaks were also observed from that of Composite-20. Notably, Composite-20 also showed a peak at 12.0° and a shoulder at about 24.5° with a lower but visible intensity, different from the pattern of silk fiber before LiBr pretreatment.

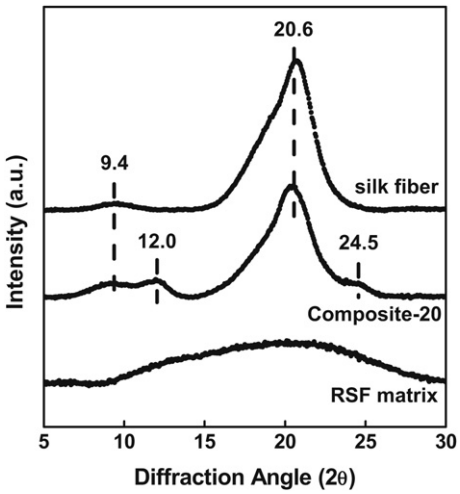

Fig. 2. X-ray diffraction patterns of RSF matrix, Composite-20 and silk fiber.

3.3. DMA results

DMA results in Fig. 3 revealed that the storage modulus E' of Composite-20 kept as high as 3 GPa with the temperature raised to 150 °C. Besides, the main tan δ peak of Composite-20 appeared at about 198 °C, between that of pure RSF matrix (179 °C) and silk fiber (219 °C). Interestingly, Composite-20 was also observed a small but broaden tan δ peak at lower temperature of about 155 °C. It should be noted that Composite-20 without LiBr pretreatment failed before 120 °C during the DMA test (not shown) probably due to the lack of adhesion between the fiber and the matrix.

3.4. Thermal properties

Thermogravimetric analysis was performed to determine the composition dependence on the thermal stability of silk fiber/

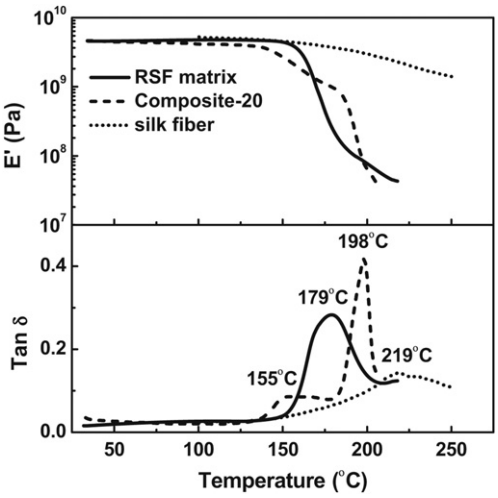

Fig. 3. DMA results of RSF matrix, Composite-20 and silk fiber.

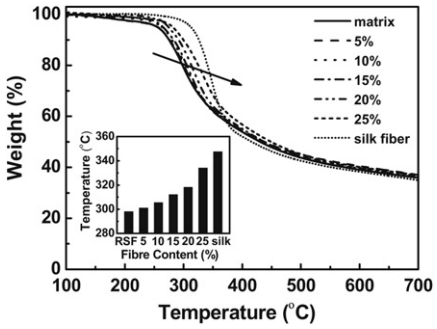

Fig. 4. TGA thermograms of RSF matrix, silk fiber and silk fiber/fibroin composites with different fiber content. Insert was the fiber content effect on the maximum thermal degradation rate temperature of the composites which was calculated from the derivative thermogravimetric (DTG) curves.

fibroin composites. In Fig. 4, the maximum thermal degradation rate of pure RSF matrix occurred at around 298 °C, much lower than that of silk fiber at 348 °C, both of which were consistent with literatures [28,29]. With the addition of silk fiber in the composites, the maximum thermal degradation rate temperature gradually increased to 334 °C when the fiber content was 25 wt%, almost approaching to that of silk fiber. Therefore, the TGA results demonstrated that, compared to that of pure RSF matrix, the thermal stability of silk fiber/fibroin composites was also improved.

4. Discussion

4.1. Effects of LiBr pretreatment on mechanical properties

The gain in mechanical performance for a composite is dependent on the compatibility between the fiber and the matrix. Even with the removal of sericin coatings [14], the compatibility of degummed silk fiber with RSF matrix is still poor [12] due to their different fine structures as mentioned before. Literatures have revealed that some chaotropic agents (e.g. LiBr [14], ternary solvent systems of $CaCl_2$–EtOH–H_2O or $Ca(NO_3)_2$–MeOH–H_2O [30,31]) or polar solvents (e.g. hexafluoroisopropanol [32], hexafluroacetone [33] or formic acid [34,35]) can break the hydrogen bonds in the fine structure of silk fiber, and reverse the well-ordered β-sheet structure back to the amorphous state, which can even result in the complete dissolution of silk fiber. Armato et al. [34,35] dissolved silkworm silk fiber in a formic acid solution and used the obtained silk 'slurry' to produce non-woven fibroin fabric. But apparently such a harsh treatment resulted in the serious strength loss of silk fiber and the devastating degradation of fibroin molecules. LiBr aqueous solution is known as a least degrading way for silk fiber dissolution [14], and only the saturated LiBr solution (ca. 9.5 mol L^{-1}) dissolves silk fiber completely while the lower LiBr concentrations (e.g. 3 mol L^{-1}) can only swell the fiber partially. Thus, a brief pretreatment of silk fiber in some moderate concentration of LiBr aqueous solution (i.e. 6 mol L^{-1}) is likely to affect the less-ordered structure on the fiber surface, and further improve the wettability and compatibility of silk fiber with RSF matrix. To show such phenomenon, the tensile stress–strain curves of Composite-20 with and without LiBr pretreatment were compared.

In Fig. 5A, the average longitudinal breaking stress and breaking elongation (i.e. in the direction parallel to the fiber array) of the LiBr-pretreated Composite-20 were 142 ± 7 MPa and 23.5 ± 1.7%, respectively, stronger and tougher than those of the untreated Composite-20 (119 ± 4 MPa and 21.4 ± 1.2%). A closer investigation on the stress–strain curves found a non-linear stress fluctuation of the untreated Composite-20 at a strain of about 2–4% (Fig. 5A insert). Considering the breaking point of pure RSF matrix at about 2% deformation and the yielding point of silk fiber at about 4% [5,6], such stress fluctuation implied a peeling of the untreated fibers from RSF matrix under tensile stress. Besides, a pronounced delamination of the untreated Composite-20 also became visible during a stretching to over 5% deformation (pointed out by white arrows in Fig. 6A). So it was likely that, as the load increased, the RSF matrix was torn off from the scaffold at 2% deformation and thereafter only the fibers were stretched, which gave a hint of no or at least weak interface adhesion in the untreated Composite-20. In contrast, neither such stress fluctuation nor stretching delamination was observed from the LiBr-pretreated Composite-20. The smooth tensile curve indicated that the composite of the LiBr-pretreated fibers and the matrix remained integral to the breaking point, which helped explain the reason for the LiBr-pretreated Composite-20 being even slightly tougher than the single silk fiber (breaking elongation about 20% [6]).

The evidence of a stronger interface adhesion between the LiBr-pretreated silk fiber and RSF matrix was provided by the transverse tensile test. Since silk fibers were uniaxially-aligned, the force was applied perpendicularly to the direction of silk fiber array during the test. Therefore, the results of the transverse tensile test determined the pulling strength of the fibers apart from RSF matrix, which in fact displayed the interface adhesion between the fiber and the matrix. As demonstrated in Fig. 5B, the untreated Composite-20 experienced a brittle fracture with a transverse breaking stress of 22 ± 1 MPa and a breaking elongation of

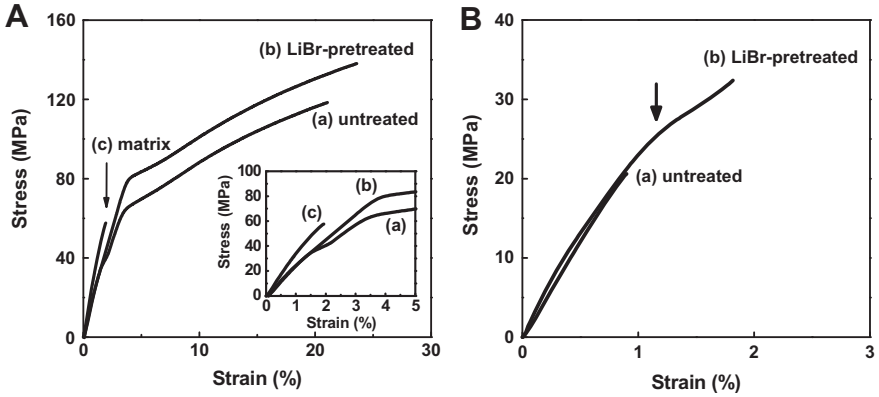

Fig. 5. Stress–strain curves of Composite-20 containing equally 20 wt% untreated (a) and LiBr-pretreated fibers (b) and RSF matrix (c) in the directions parallel (A) and perpendicular (B) to the fiber array, respectively.

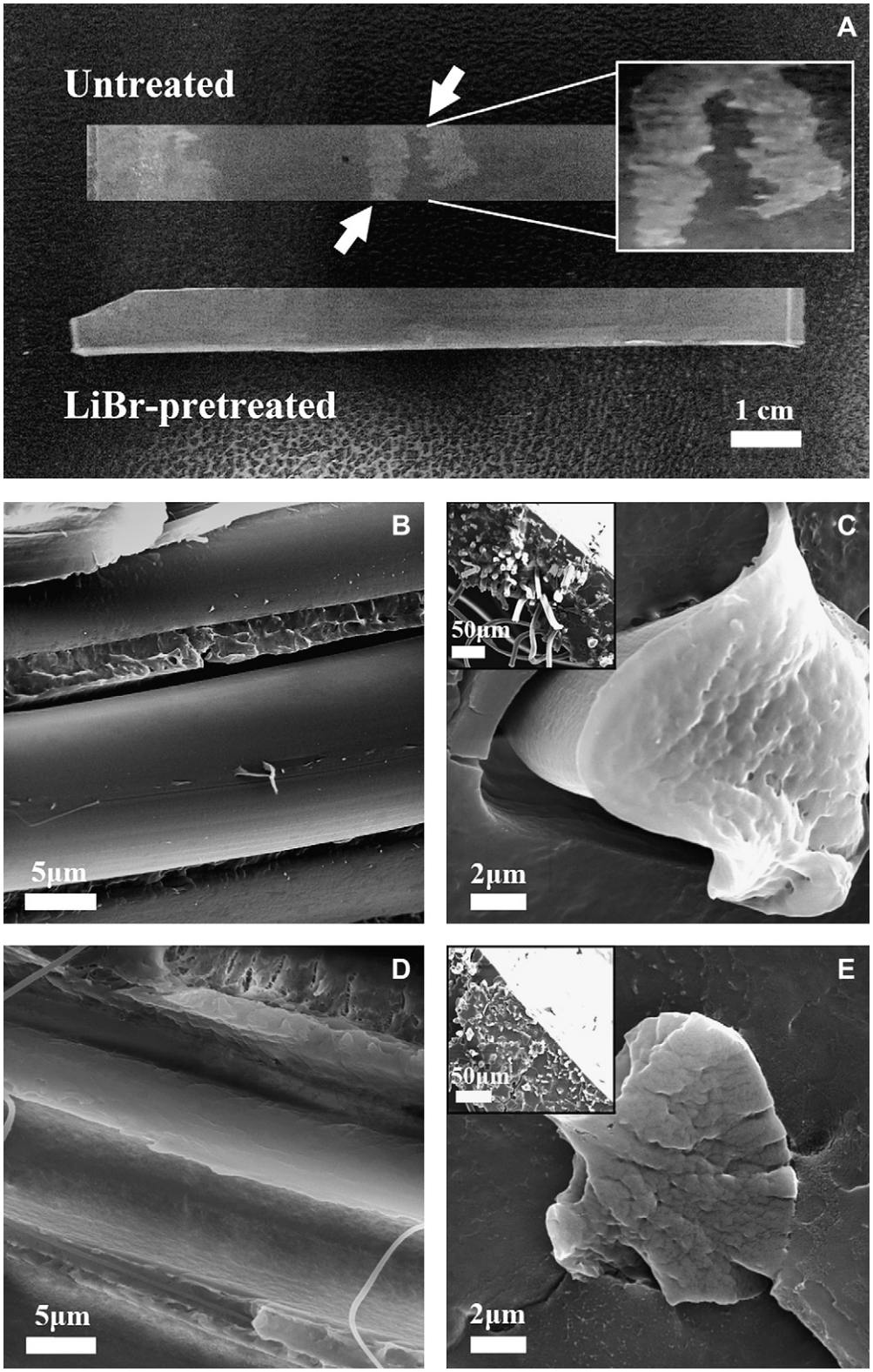

Fig. 6. (A): Photograph of Composite-20 after stretching to over 5% deformation. (B–E): SEM images of the fracture section of silk fiber/fibroin composites after tensile test in the directions perpendicular (B & D) and parallel (C & E) to the fiber array. (B & C) and (D & E) were prepared with the untreated and LiBr-pretreated fibers, respectively.

1.0 ± 0.1%, respectively. In contrast, the LiBr-pretreated Composite-20 was likely to show a yielding point in the stress–strain curve (pointed out by black arrow in Fig. 5B). Also the stronger transverse breaking stress (32 ± 3 MPa) and more extensibility (1.9 ± 0.3%) of the composite indicated the enhancement of interface adhesion between silk fiber and RSF matrix via 6 mol L^{-1} LiBr pretreatment. However, it should be noted that although the transverse breaking stress was much weaker than the longitudinal one due to the

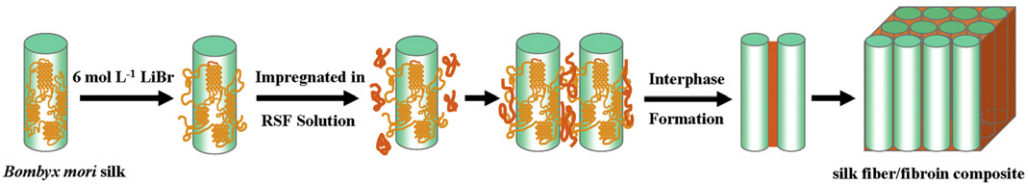

Scheme 1. Proposed preparation process of silk fiber/fibroin composites via LiBr pretreatment for the improvement of interface adhesion between silk fiber and RSF matrix.

orientation of silk fiber array, this limit could be overcome by arranging a cross-layer framework of the uniaxially-aligned silk fibers before LiBr pretreatment.

Furthermore, previous studies showed that LiBr aqueous solutions with different concentrations (e.g. 6 mol L^{-1} vs. 9.5 mol L^{-1}) would disrupt the fine structure of silk fiber to different degrees [36]. Therefore, we also attempted the pretreatment on silk fiber by the saturated LiBr solution (ca. 9.5 mol L^{-1}) for the same incubation time (10 min). Although good compatibility between silk fiber and RSF matrix was found by SEM, the mechanical properties of the composite were relatively poorer, with a breaking stress of 100 ± 6 MPa and a breaking elongation of 19.6 ± 1.6% (Electronic Supplementary Material, Fig. S1). It indicated that despite the relatively short incubation time, this pretreatment did affect a larger part of β-sheet structure (or well-ordered domains) in silk fiber and therefore caused a loss in the fiber qualities.

4.2. Effects of LiBr pretreatment on fracture section morphologies

The adhesion between silk fiber and RSF matrix was also visually assessed by the fracture sections of silk fiber/fibroin composites. After the failure of the composite, the untreated fibers showed a smooth surface completely devoid of the RSF matrix (Fig. 6B and C), indicating an early failure at the interface followed by a large quantity of fibers pulling out of the matrix (Fig. 6C, inserted image). In contrast, the LiBr-pretreated fibers displayed a rough surface (Fig. 6D), and most of them were stretched to break together with RSF matrix simultaneously (Fig. 6E) rather than being only pulled out from the matrix. This suggested a good compatibility between the LiBr-pretreated silk fiber and RSF matrix, and might explain the increased strength of silk fiber/fibroin composites. Moreover, the resulted fault fissures and folds surrounding the slit tip of the fiber and the matrix (Fig. 6E) may be seen as a toughening proof of the LiBr-pretreated composites.

4.3. Mechanism of interface enhancement via LiBr pretreatment

Considering the solubility of silk fiber in response to LiBr aqueous solution, Gido et al. [37] studied the ternary phase diagram of LiBr–H_2O–fibroin and believed that a less-ordered fibroin structure (vs. β-sheet structure termed Silk II) occurred in the system containing 5–7 mol L^{-1} LiBr. As revealed in Fig. 2, the XRD results of the LiBr-pretreated Composite-20 showed a new peak at 12.0° and a shoulder at about 24.5° that were different from the XRD patterns of either RSF matrix or silk fiber. Similar XRD patterns were also found by Kaplan et al. [38] in spin-coating RSF films, and were explained as a co-existence of the amorphous and less-ordered domains together and were different from the Silk II form. Besides, the DMA results in Fig. 3 showed that a broad tan δ peak appeared at around 155 °C for the LiBr-pretreated Composite-20. In our opinion, this new relaxation peak at the relatively lower temperature also implied the presence of some less-ordered silk fibroin structure in the composite after LiBr pretreatment, which was consistent with the XRD analysis and could explain together the interface enhancement mechanism of silk fiber/fibroin composites via LiBr pretreatment.

As shown in Scheme 1, the interface enhancement mechanism was like a result of following events: At first, 6 mol L^{-1} LiBr partially swelled and loosened the relatively less-ordered structures on the smooth but insoluble fiber surface without significant disruption to the fiber's bulky mechanical properties. Then as the LiBr-pretreated fibers were impregnated in RSF matrix, these loosened fibroin segments on the fiber surface were penetrated and entangled with the fibroin coils in the aqueous solution, and formed a fibroin interphase. This produced interphase served as mechanical interlocking with both the fibers and RSF matrix to improve the interface adhesion between them, and therefore resulted in a silk fiber/fibroin composite with good mechanical and thermal performance.

5. Conclusions

A moderate LiBr pretreatment was found to improve the impregnation of degummed silk fiber in RSF matrix, with little damage to the fiber's original properties. The enhanced adhesion between the pretreated silk fiber and RSF matrix resulted in a silk fiber/fibroin composite with the excellent portfolio of mechanical and thermal properties, much better than those of the pure RSF counterpart. Therefore, with the diversity of silks from insects and spiders, this feasible, versatile and eco-friendly LiBr pretreatment method may help the exploitation of animal silk based materials with promising properties for various applications.

Acknowledgement

This work was supported by the National Natural Science Foundation of China (NSFC 20525414), 973 Project of Chinese Ministry of Science and Technology (No. 2009CB930000), the Program for New Century Excellent Talents in University of MOE of China (NCET 060354), and the Program for Changjiang Scholars and Innovative Research Team in Fudan University. The authors further thank Dr. Yong Yang for DMA test of silk fiber, and Prof. Qiangguo Du and Mr. Changjie Ge of Fudan University for the technical support of fiber reeling machine. Special thanks to Dr. Alexander Sponner and Dr. Junjie Wu for their critical reading and polishing the English.

Appendix. Supplementary material

Supplementary data associated with this article can be found, in the online version, at doi:10.1016/j.polymer.2010.08.042.

References

[1] Nishino T. Green composites: polymer composites and the environment. CPC Press; 2004. p. 49–80.
[2] Netravali AN, Chabba S. Materials Today 2003;6(4):22–9.
[3] Peijs T. Materials Today 2003;6(4):30–5.
[4] Porter D, Vollrath F. Advanced Materials 2009;21(4):487–92.
[5] Shao ZZ, Vollrath F. Nature 2002;418(6899):741.
[6] Zhou GQ, Shao ZZ, Knight DP, Yan JP, Chen X. Advanced Materials 2009;21(3):366–70.
[7] Lee SM, Cho D, Park WH, Lee SG, Han SO, Drzal LT. Composites Science and Technology 2005;65(3–4):647–57.
[8] Kim HS, Park BH, Yoon JS, Jin HJ. Polymer International 2007;56(8):1035–9.
[9] Li W, Qiao XY, Sun K, Chen XD. Journal of Applied Polymer Science 2008;110(1):134–9.

[10] Cheung HY, Lau KT, Tao XM, Hui D. Composites Part B-Engineering 2008;39 (6):1026–33.
[11] Setua DK, Dutta B. Journal of Applied Polymer Science 1984;29:3097–114.
[12] Li M, Lu S. PRC Patent 02138127.5; 2002.
[13] Shao Z, Vollrath F, Sirichaisit J, Young RJ. Polymer 1999;40(10):2493–500.
[14] Chen X, Knight DP, Shao ZZ, Vollrath F. Polymer 2001;42(25):9969–74.
[15] Chen X, Knight DP, Shao ZZ, Vollrath F. Biochemistry 2002;41(50):14944–50.
[16] Mayes EL, Vollrath F, Mann S. Advanced Materials 1998;10(10):801–5.
[17] Wright DD, Lautenschlager EP, Gilbert JL. Journal of Biomedical Materials Research 1997;36(4):441–53.
[18] Nishino T, Matsuda I, Hirao K. Macromolecules 2004;37(20):7683–7.
[19] Gandini A, Curvelo AAD, Pasquini D, de Menezes AJ. Polymer 2005;46(24): 10611–3.
[20] Qi HS, Cai J, Zhang LN, Kuga S. Biomacromolecules 2009;10(6):1597–602.
[21] Chen X, Shao Z, Zhou L. PRC Patent 03142201.2; 2003.
[22] Shao Z, Yuan Q, Chen X. PRC Patent 200710171825.X; 2007.
[23] Yang Y, Chen X, Shao ZZ, Zhou P, Porter D, Knight DP, et al. Advanced Materials 2005;17(1):84–8.
[24] Vepari C, Kaplan DL. Progress in Polymer Science 2007;32(8–9):991–1007.
[25] Hardy JG, Romer LM, Scheibel TR. Polymer 2008;49(20):4309–27.
[26] Wang YZ, Kim HJ, Vunjak-Novakovic G, Kaplan DL. Biomaterials 2006;27 (36):6064–82.
[27] Krejchi MT, Cooper SJ, Deguchi Y, Atkins EDT, Fournier MJ, Mason TL, et al. Macromolecules 1997;30(17):5012–24.
[28] Motta A, Fambri L, Migliaresi C. Macromolecular Chemistry and Physics 2002;203(10–11):1658–65.
[29] Porter D, Vollrath F, Tian K, Chen X, Shao ZZ. Polymer 2009;50(7):1814–8.
[30] Li MZ, Lu SZ, Wu ZY, Yan HJ, Mo JY, Wang LH. Journal of Applied Polymer Science 2001;79(12):2185–91.
[31] Li MZ, Wu ZY, Zhang CS, Lu SZ, Yan HJ, Huang D, et al. Journal of Applied Polymer Science 2001;79(12):2192–9.
[32] Liivak O, Blye A, Shah N, Jelinski LW. Macromolecules 1998;31(9):2947–51.
[33] Ohgo K, Zhao CH, Kobayashi M, Asakura T. Polymer 2003;44(3):841–6.
[34] Armato U, Dal Pra I, Kesenci K, Migliaresi C, Motta A. WO 02/29141 A1; 2002.
[35] Unger RE, Wolf M, Peters K, Motta A, Migliaresi C, Kirkpatrick CJ. Biomaterials 2004;25(6):1069–75.
[36] Cheng C, Yang YH, Chen X, Shao ZZ. Chemical Communications 2008;43:5511–3.
[37] Sohn S, Strey HH, Gido SP. Biomacromolecules 2004;5(3):751–7.
[38] Jiang CY, Wang XY, Gunawidjaja R, Lin YH, Gupta MK, Kaplan DL, et al. Advanced Functional Materials 2007;17(13):2229–37.